

## Metal Substrate Engineering to Modulate CO<sub>2</sub> Hydrogenation to Methanol on Inverse Zr<sub>3</sub>O<sub>6</sub>/CuPd Catalysts

Bin Qin<sup>a#</sup>, XiaoYing Sun<sup>a#</sup>, Jianzhuo Lu<sup>a</sup>, Zhen Zhao<sup>a,b\*</sup>, Bo Li<sup>a\*</sup>

<sup>a</sup>Institute of Catalysis for Energy and Environment, College of Chemistry and Chemical Engineering, Shenyang Normal University, Shenyang 110034, China

<sup>b</sup>State Key Laboratory of Heavy Oil Processing, China University of Petroleum, Beijing, 102249, China

Corresponding Authors:

\* B. Li: e-mail, boli@synu.edu.cn

\* Z. Zhao: email, zhenzhao@cup.edu.cn or zhaozhen1586@163.com

#: These authors contributed equally to this work

**Table S1** The details of setup for construction of Z/CuPd models.

parameters catalysts	Supercell	Atom Layers	Fixed Layers	Vacuum Gap
Z/CuPd(100)-Cu	5×5	4	bottom 2	12Å
Z/CuPd(100)-Pd	5×5	4	bottom 2	12Å
Z/CuPd(110)	5×4	4	bottom 2	11Å
Z/CuPd(111)-Cu	4×4	8	bottom 4	12Å
Z/CuPd(111)-Pd	4×4	8	bottom 4	12Å

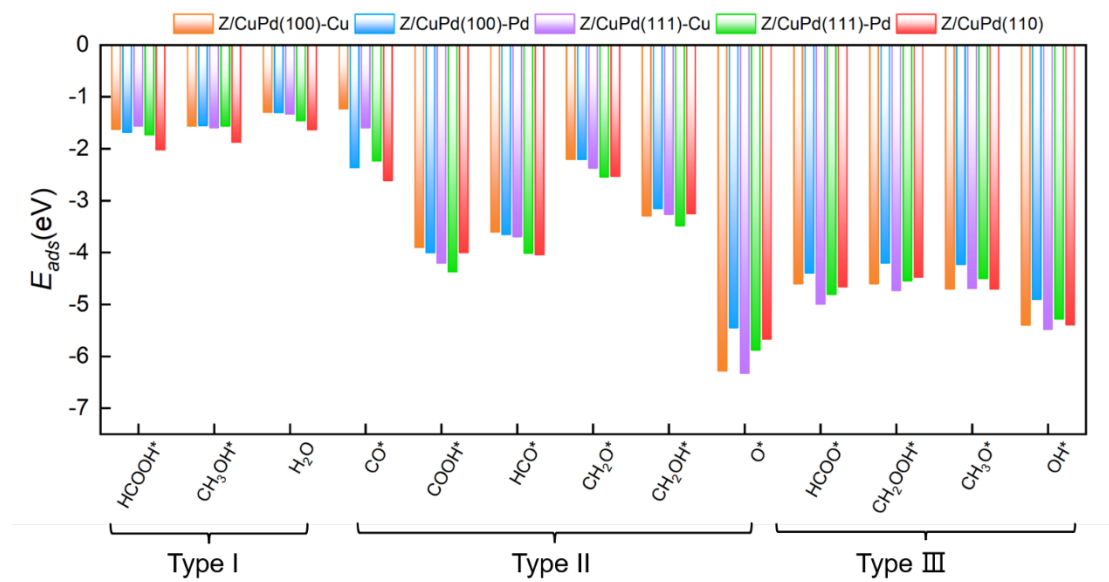
**Table S2** Bader charge analysis(in |e|) of CO<sub>2</sub> adsorbed on Zr<sub>3</sub>O<sub>6</sub>/CuPd catalysts.

	Z/CuPd(100) -Cu	Z/CuPd(100) -Pd	Z/CuPd(110)	Z/CuPd(111) - Cu	Z/CuPd(110) - Pd
O <sub>1</sub> (Zr)	-1.10	-1.12	-1.12	-1.11	-1.11
O <sub>2</sub> (CuPd)	-1.04	-1.00	-1.07	-1.04	-1.02
C	1.22	1.44	1.45	1.45	1.56
total	-0.92	-0.68	-0.74	-0.70	-0.57

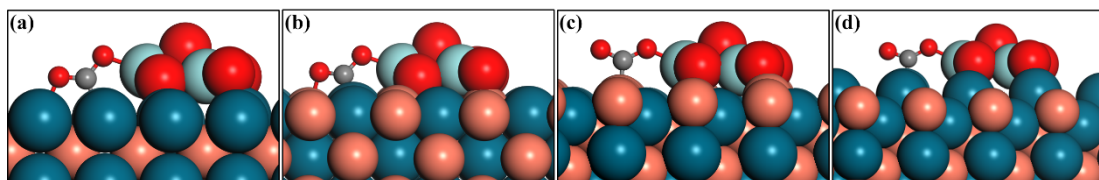
**Table S3** Adsorption energies of key intermediates involved in methanol synthesis progress over Zr<sub>3</sub>O<sub>6</sub>/CuPd catalysts.

species catalysts	Z/CuPd(100)- Cu	Z/CuPd(100)- Pd	Z/CuPd(110)	Z/CuPd(111)- Cu	Z/CuPd(111)- Pd
H	-2.86	-2.72	-2.90	-2.82	-2.85
O	-6.28	-5.45	-5.67	-6.32	-5.88
H <sub>2</sub>	-0.31	-0.33	-0.44	-0.37	-0.50
CO <sub>2</sub>	-1.51	-1.65	-1.67	-1.42	-1.73

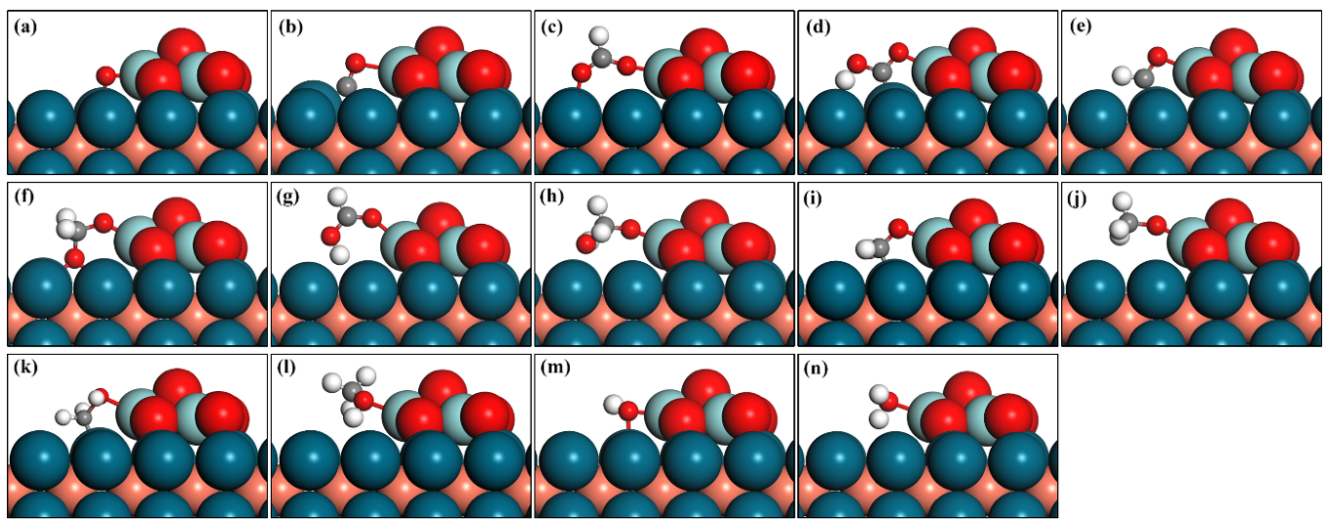
CO	-1.23	-2.36	-2.61	-1.59	-2.23
OH	-5.47	-4.95	-5.39	-5.48	-5.28
HCOO	-4.65	-4.39	-4.66	-4.99	-4.81
COOH	-3.93	-4.00	-4.00	-4.20	-4.37
HCOOH	-1.62	-1.68	-2.02	-1.56	-1.73
CH <sub>2</sub> OOH	-4.63	-4.26	-4.47	-4.73	-4.54
HCO	-3.60	-3.65	-4.04	-3.69	-4.01
CH <sub>2</sub> O	-2.20	-2.20	-2.53	-2.37	-2.54
CH <sub>3</sub> O	-4.75	-4.23	-4.70	-4.69	-4.50
CH <sub>2</sub> OH	-3.29	-3.15	-3.25	-3.26	-3.48
CH <sub>3</sub> OH	-1.56	-1.55	-1.87	-1.59	-1.56
H <sub>2</sub> O	-1.29	-1.30	-1.63	-1.33	-1.46



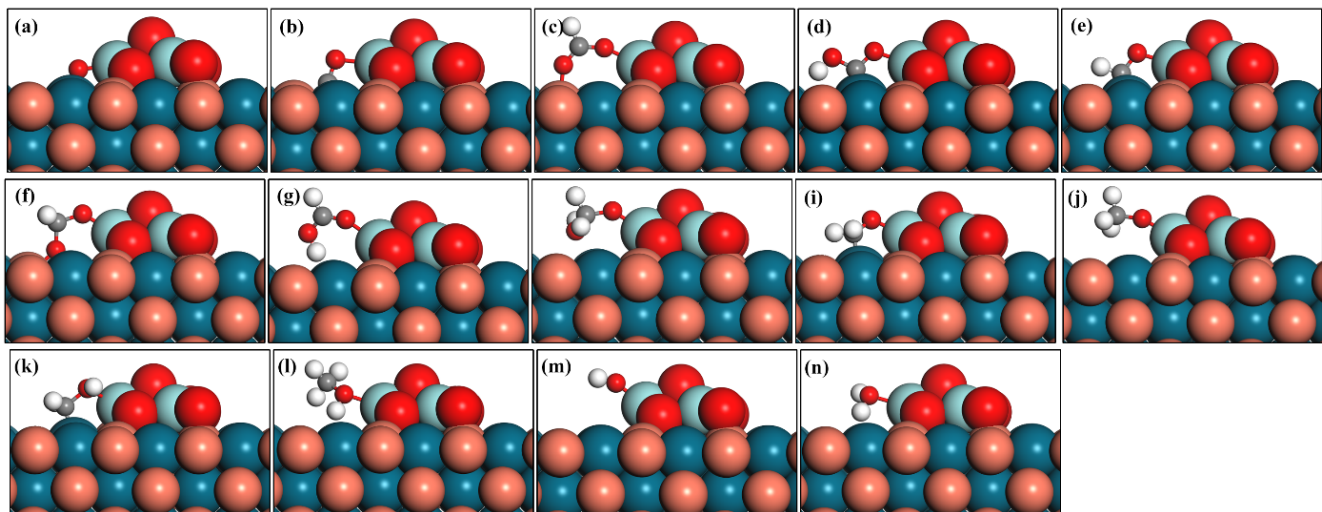
**Figure S1** Histogram of adsorption energies of key intermediates in the methanol synthesis process.



**Figure S2** DFT optimized geometry configuration of CO<sub>2</sub> adsorbed on (a) Z/CuPd(100)-Pd (b) Z/CuPd(110) (c) Z/CuPd(111)-Cu (d) Z/CuPd(111)-Pd

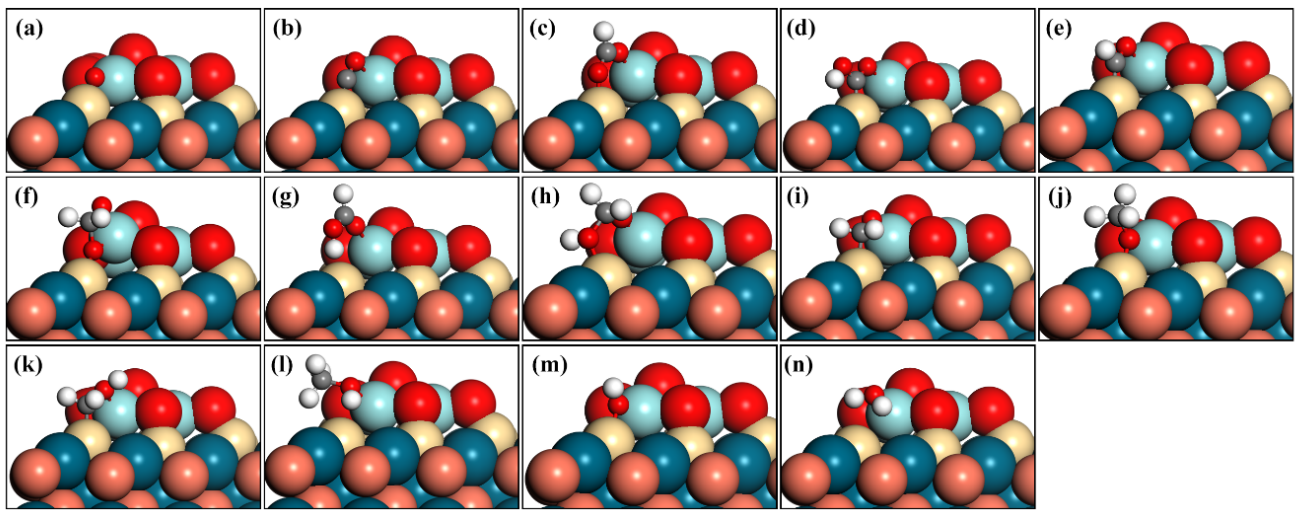


**Figure S3** Side views of the optimized structures of key intermediates adsorbed on ZnPdCu(100)-Pd (a) O\* (b) CO\* (c) HCOO\* (d) COOH\* (e) HCO\* (f) CH<sub>2</sub>OO\* (g) HCOOH\* (h) CH<sub>2</sub>OOH\* (i) CH<sub>2</sub>O\* (j) CH<sub>3</sub>O\* (k) CH<sub>2</sub>OH\* (l) CH<sub>3</sub>OH\* (m) OH\* (n) H<sub>2</sub>O\*

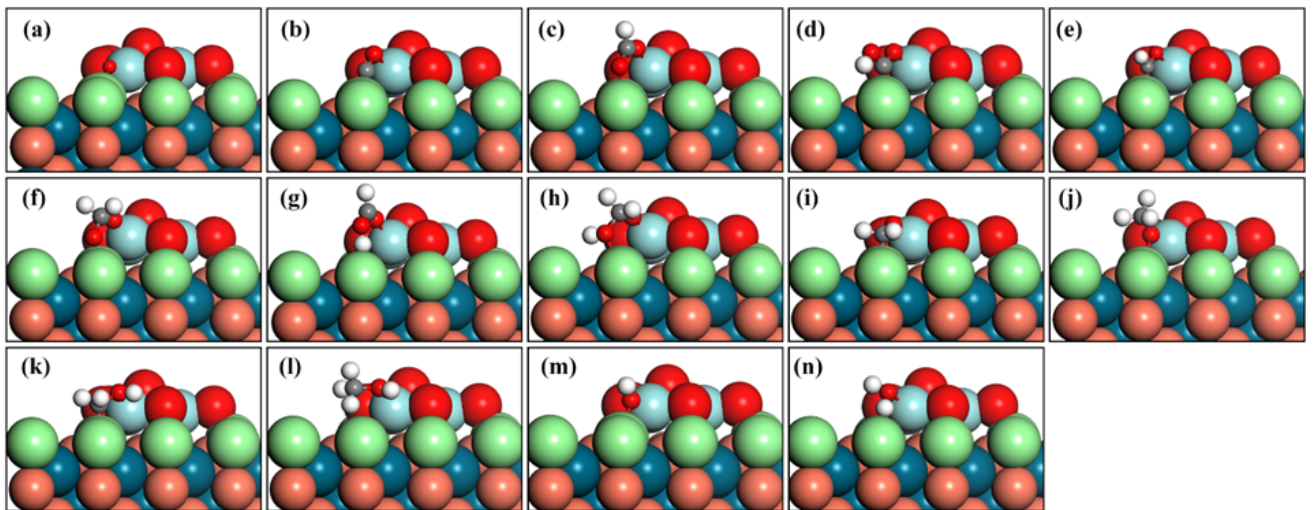


**Figure S4** Side views of the optimized structures of key intermediates adsorbed on ZnPdCu(110)

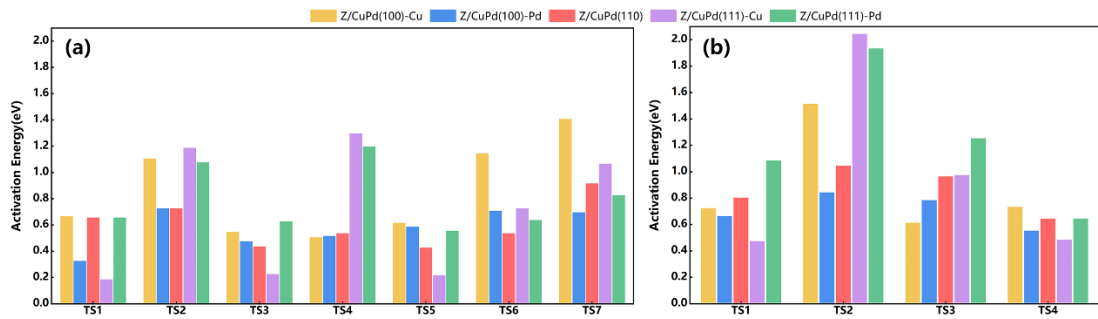
$\text{CH}_2\text{O}^*$  (j)  $\text{CH}_3\text{O}^*$  (k)  $\text{CH}_2\text{OH}^*$  (l)  $\text{CH}_3\text{OH}^*$  (m)  $\text{OH}^*$  (n)  $\text{H}_2\text{O}^*$



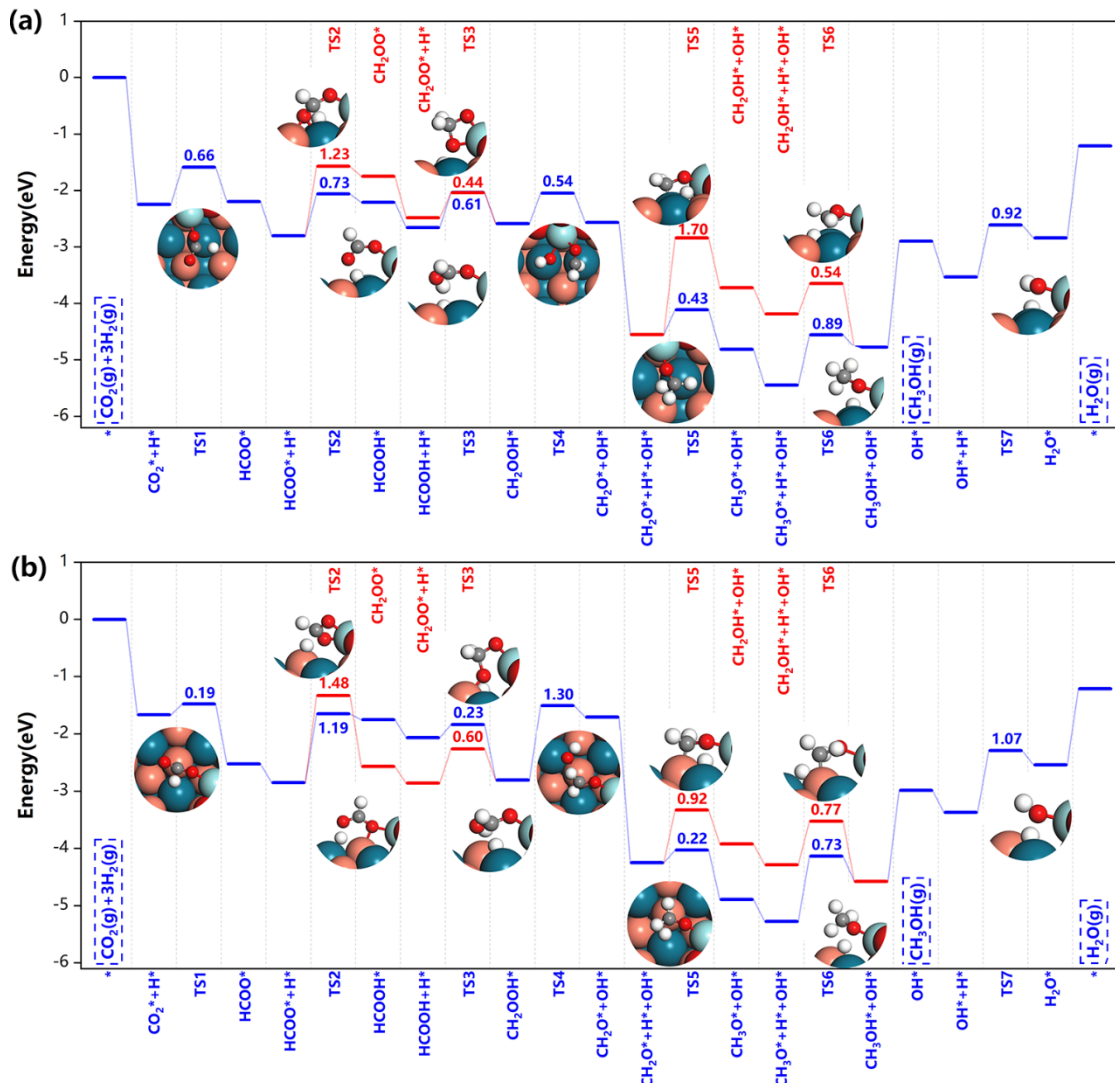
**Figure S5** Side views of the optimized structures of key intermediates adsorbed on Z/PdCu(111)-Cu (a)  $\text{O}^*$  (b)  $\text{CO}^*$  (c)  $\text{HCOO}^*$  (d)  $\text{COOH}^*$  (e)  $\text{HCO}^*$  (f)  $\text{CH}_2\text{OO}^*$  (g)  $\text{HCOOH}^*$  (h)  $\text{CH}_2\text{OOH}^*$  (i)  $\text{CH}_2\text{O}^*$  (j)  $\text{CH}_3\text{O}^*$  (k)  $\text{CH}_2\text{OH}^*$  (l)  $\text{CH}_3\text{OH}^*$  (m)  $\text{OH}^*$  (n)  $\text{H}_2\text{O}^*$

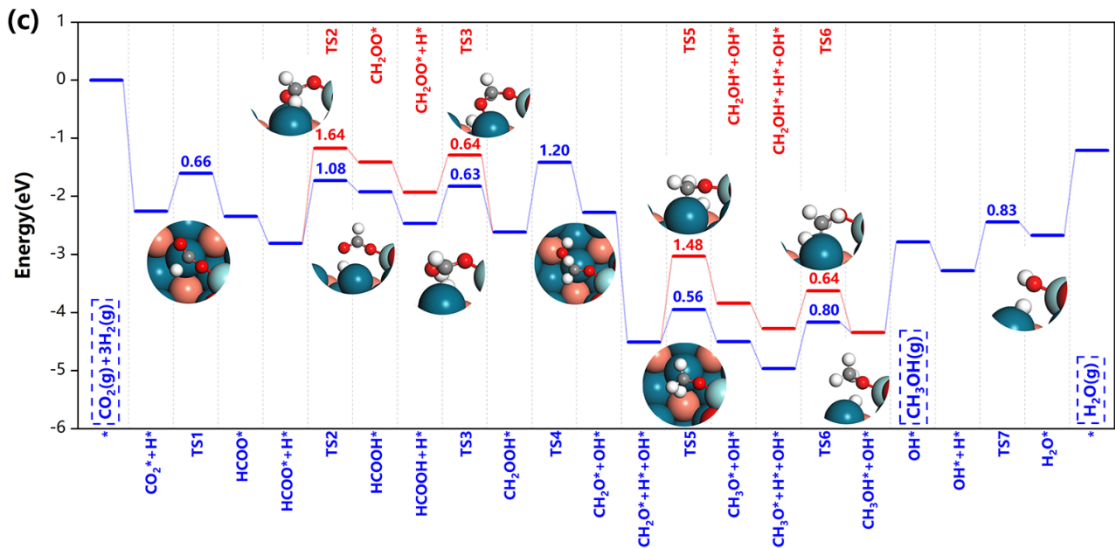


**Figure S6** Side views of the optimized structures of key intermediates adsorbed on Z/PdCu(111)-Pd (a)  $\text{O}^*$  (b)  $\text{CO}^*$  (c)  $\text{HCOO}^*$  (d)  $\text{COOH}^*$  (e)  $\text{HCO}^*$  (f)  $\text{CH}_2\text{OO}^*$  (g)  $\text{HCOOH}^*$  (h)  $\text{CH}_2\text{OOH}^*$  (i)  $\text{CH}_2\text{O}^*$  (j)  $\text{CH}_3\text{O}^*$  (k)  $\text{CH}_2\text{OH}^*$  (l)  $\text{CH}_3\text{OH}^*$  (m)  $\text{OH}^*$  (n)  $\text{H}_2\text{O}^*$

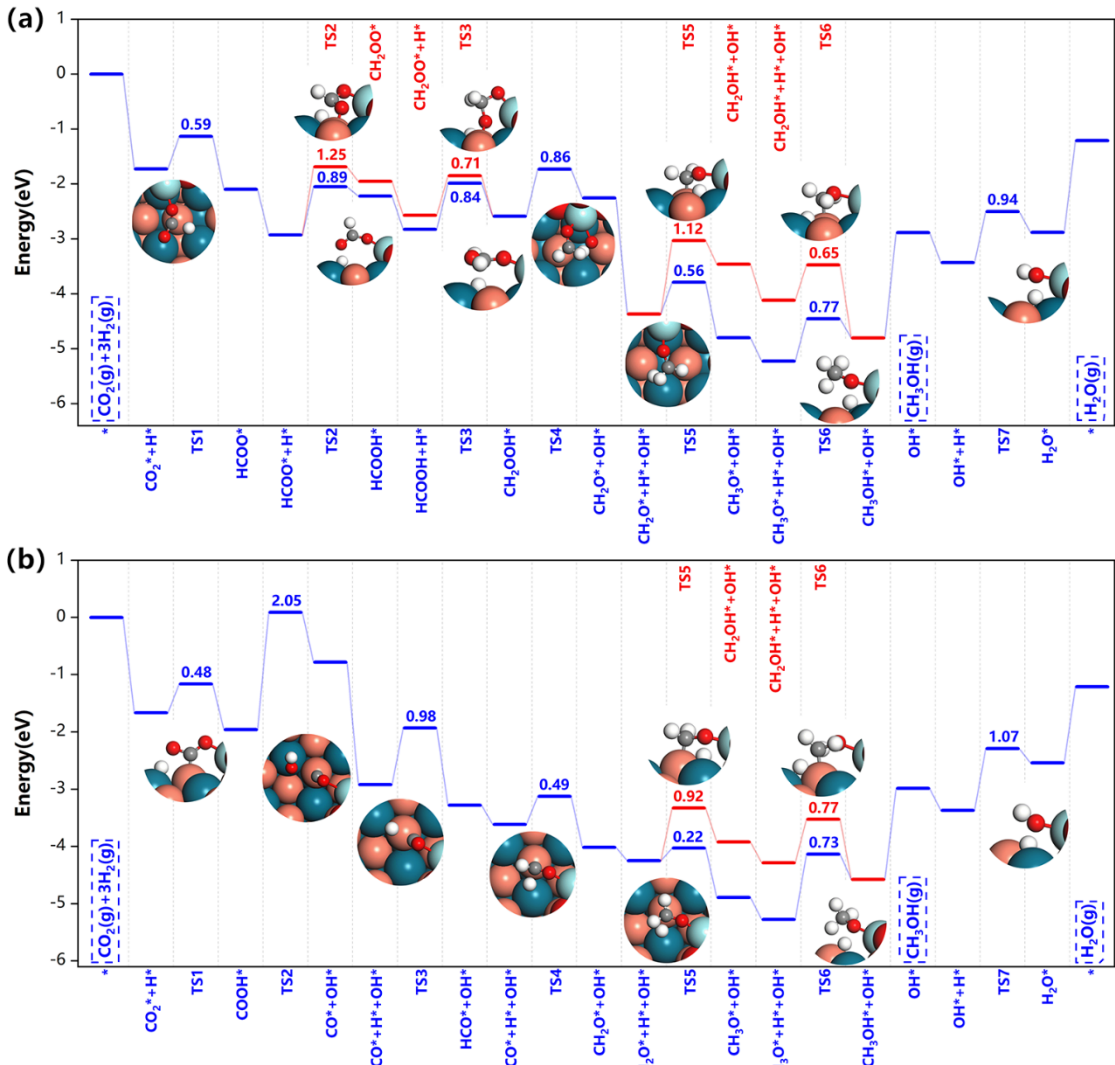


**Figure S7** The lowest energy barrier along (a) Formate pathway (b) RWGS+CO-hydro pathway.





**Figure S8** Potential energy diagrams and corresponding transition state structures of methanol formation over (a) Z/CuPd(110) (b) Z/CuPd(111)-Cu (c) Z/CuPd(111)-Pd along formate pathway.



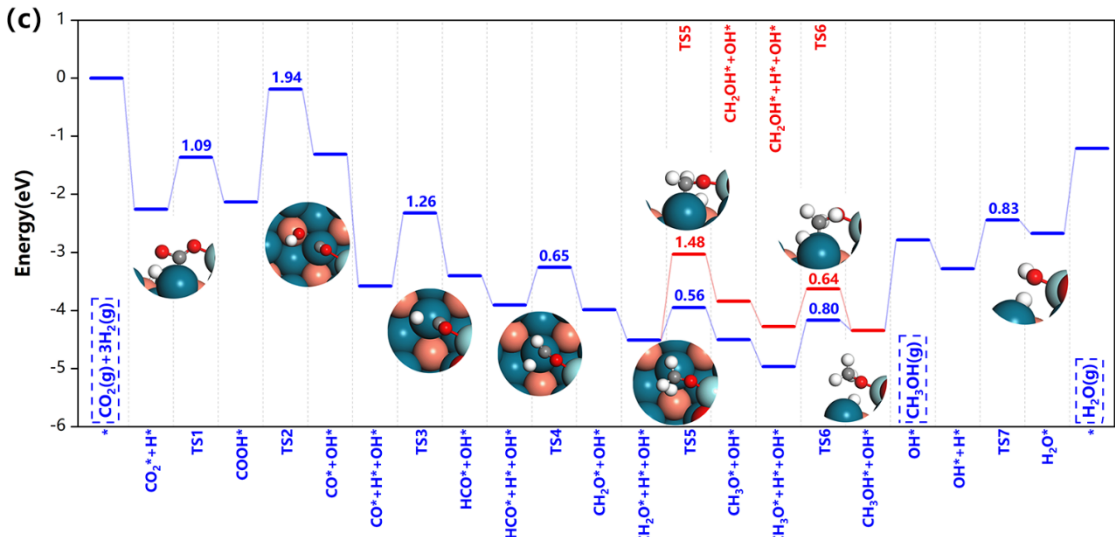


**Figure S9** Potential energy diagrams and corresponding transition state structures of methanol formation over (a) Z/CuPd(110) (b) Z/CuPd(111)-Cu (c) Z/CuPd(111)-Pd along RWGS + CO-hydro pathway.

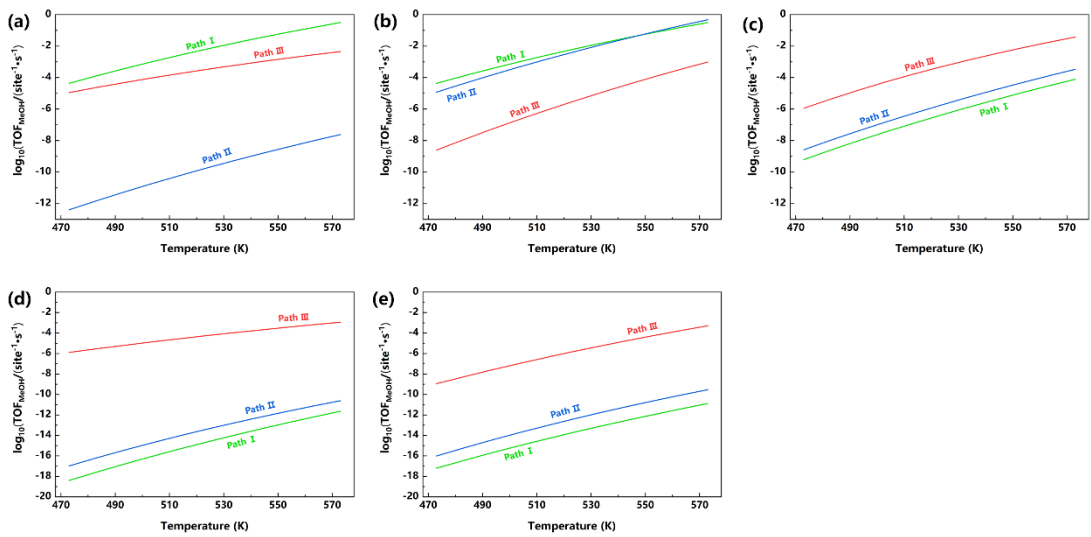


**Figure S10** The calculated logarithm turnover frequency (TOF) of MeOH formation pathways over (a) Z/CuPd(100)-Cu (b) Z/CuPd(100)-Pd (c) Z/CuPd(110) (d) Z/CuPd(111)-Cu and (e) Z/CuPd(111)-Pd at reactant pressure of 5 bar.

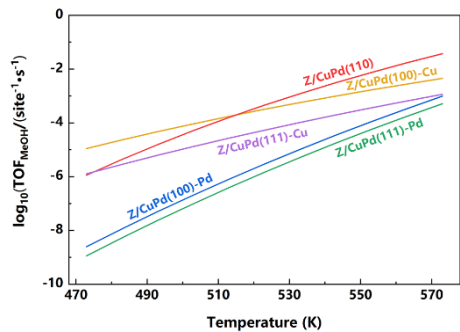


**Figure S11** The logarithm turnover frequency (TOF) of  $\text{CO}_2$  direct activation pathway over Zr<sub>3</sub>O<sub>6</sub>/CuPd catalysts.